

The synthesis and characterization of titanium silicalite-1

Y. G. LI*, Y. M. LEE, J. F. PORTER‡

Department of Chemical Engineering, Hong Kong University of Science & Technology, Clear Water Bay, Hong Kong SAR, People's Republic of China
E-mail: kejep@ust.hk

This paper investigates the effect of the variation in alkoxide precursor ratio and templating agent concentration on the production of titanium silicalite (TS-1) through analysis using various physical characterisation techniques. X-ray diffraction showed clear evidence for the MFI zeolite structure and a high degree of crystallinity in all systems. For those materials prepared using a templating agent with ultra low alkali metal content, excellent agreement with previously reported unit cell parameters was obtained. For these same systems, 20% higher specific surface areas were also obtained by nitrogen adsorption. Analysis using an energy dispersive x-ray spectrometer coupled to a scanning electron microscope showed that the product typically contained between 60 and 90% of the titanium in the precursor and some dependence of titanium incorporation on the initial mixture composition was also observed. The results from Raman spectroscopy indicated titanium incorporation into the silicalite framework for all systems. For those materials produced using a templating agent with low alkali metal content, extra-framework anatase titanium dioxide was also identified at moderate Ti:Si mole ratios (>0.03) in the initial mixture. Due to its lower penetration depth, x-ray photoelectron spectroscopy (XPS) was used to characterise the titanium species in the surface layer. The XPS results indicated that a small amount of extra-framework titania was present in the surface of most of the TS-1 samples and the proportion of extra-framework material was observed to increase with both precursor alkali metal content and precursor titanium to silicon ratio. © 2002 Kluwer Academic Publishers

1. Introduction

In the years since Taramasso and co-workers first synthesised the zeolite titanium silicalite (TS-1) [1], this material has attracted a great deal of attention. Structurally, the titanium in TS-1 isomorphously replaces silicon in a tetrahedral site of the MFI silicalite lattice. As such, it combines the advantages of the high coordination ability of Ti^{4+} ions with the hydrophobicity of the silicalite framework, while retaining the spatial selectivity and specific local geometry of the active sites of the molecular sieve structure. This combination reveals unique selective catalytic properties for a broad range of oxidations with hydrogen peroxide, such as the hydroxylation of phenol [2], the ammoximation of cyclohexanone [3], the epoxidation of olefins [4] and the oxidation of saturated hydrocarbons [5] and alcohols [8].

The titanium in silicalite framework sites is proposed to form a five-membered cyclic structure, combining a titanium hydroperoxo moiety (Ti-OOH) and a protic molecule at the Ti sites, which has been suggested as the active species for epoxidation of lower olefins with hydrogen peroxide [16]. The activation of H_2O_2 on the titanyl group by formation of titanium peroxo com-

plexes has also been proposed for the ammoximation reaction mechanism [6].

Although some researchers have observed that increasing the titanium content of TS-1 enhances its catalytic activity [17], there is a limit to the possible extent of incorporation of titanium into the tetrahedral framework. Theoretically, the larger size of its ionic radius precludes titanium incorporation in the lattice of the silicalite structure—however, in practice tetravalent titanium is usually present in an octahedral coordination. The synthesis of materials containing isolated tetrahedral Ti is rather difficult given its strong tendency to polymerize in aqueous systems—especially at the high pH conditions normally encountered in TS-1 synthesis—often resulting in the formation of separate, stable, titanium dioxide phases. The maximum mole fraction of titanium incorporated in TS-1 framework reported in the original patent was 0.025, which corresponds to approximately 2.5 Ti per unit cell [1]. Other researchers have reported higher values: van der Pol *et al.* claimed an upper limit for $Ti/(Ti + Si)$ of 0.04 [7], Tuel *et al.* reported TS-1 with more than 5 Ti per unit cell [25] and Thangaraj *et al.* reported TS-1 with a

*Present Address: School of Chemistry and Chemical Engineering, Zhongshan University, Guangzhou, People's Republic of China.

‡Author to whom all correspondence should be addressed.

titanium content of up to 8.5 mole percent by a modified synthesis method [9]. Criticism of research reporting high levels of titanium incorporation generally centres on the extent and detail of characterisation of the Ti species, suggesting that much of the material is actually present as extra-framework Ti [10]. Indeed, there is significant difficulty preventing TiO₂ from precipitating during crystallization when the synthesis solution contains over 2 weight percent titanium. The presence of extra-framework titanium dioxide significantly lowers the catalytic activity of the material because of its high activity for the decomposition of hydrogen peroxide to water and oxygen [11] as well as the possibility of the TiO₂ blocking access of reacting molecules to the internal active framework Ti⁴⁺ sites [12]. Consequently, the location of the titanium ions in framework or extra-framework positions and their coordination in the molecular sieves are interesting not only from a structural point of view but also in connection with the mechanism of the catalytic transformations.

A number of physical characterization techniques have been applied in identifying the state and coordination of titanium in TS-1, such as XRD [10, 13, 35], IR and Raman [13–15, 33–35], XPS [15, 41], XANES [12, 21, 22, 32, 41], EXAFS [18, 22, 32, 41], UV-visible Diffuse Reflectance [31, 33–35], ESR [34] and NMR [13, 35]. Despite some significant successes in this area, a consensus has yet to be achieved over the correct interpretation of certain spectroscopic data. For example, most authors have used the increase of the intensity of IR and Raman bands close to 960 cm⁻¹ as evidence of incorporation of Ti in the silicalite framework. Indeed, although there is general agreement that these peaks are associated with the presence of framework Ti [34, 35], discussion continues as to whether this peak results from perturbation of the vibration modes of two non-bridging oxygens by the presence of Ti⁴⁺ in a neighboring position [15] or the asymmetric stretching modes of Si–O–Ti bridges [33]. Further evidence for titanium incorporation in the silicalite framework is provided from XRD patterns, which not only confirm the crystalline molecular sieve structure but also demonstrate changes in the unit cell parameters with titanium content. A linear dependence on Ti content was observed for expansion of unit cell volume in titanium-substituted silicalites from which the tetrahedral coordination of the titanium in the TS-1 framework was proposed [10, 13]. Although other researchers have reported a similar linear relationship of the TS-1 unit cell volume with titanium content extending up to 10 Ti per unit cell [9], the determination of the unit cell parameters strongly depends on the procedure used, especially the number of selected reflections [20].

The determination of the exact amount of the extra-framework titanium is more difficult. A number of experimental methods provide qualitative information about the presence of extra-framework Ti in zeolite samples—e.g. Raman spectroscopy can identify anatase and rutile titania impurities present in TS-1 at concentrations below 1 weight percent and from XPS, the ratio of the peaks of binding energy corresponding to framework and extraframework Ti can be used

to estimate the composition of the surface layer of the zeolites. Several researchers have used combinations of characterisation techniques in order to attempt to locate and quantify the Ti species present. Trong On *et al.* suggested that most titanium ions are sited in non-substitutional framework sites according to their investigation by FT-IR, XPS, XANES and EXAFS [21]. XANES and EXAFS investigations by Behrens *et al.* indicated that Ti was mainly octahedrally coordinated in their TS-1 sample, even though small but measurable amounts of tetrahedral and square pyramidal Ti were detected [22]. Such contrasting observations indicate that the complete qualitative and quantitative characterization of titanium incorporation in the silicalite framework remains a challenging task. A comprehensive review of the characterisation of titanium silicalites was recently produced by Vayssilov [23].

In the present work a series of TS-1 samples were synthesized under different conditions. The samples have been characterized using XRD, SEM-EDX, Raman, XPS, and BET N₂ adsorption. The purpose of the work is to attempt to provide further understanding of the incorporation efficiency, location and the coordination states of titanium species in TS-1.

2. Method and materials for TS-1 zeolite synthesis

The synthesis procedure used in this work is similar to that presented by van der Pol and van Hooff [7]. The alkoxide precursors used were tetraethyl orthosilicate (TEOS) and tetraethyl orthotitanate (TEOT), both supplied by Aldrich Chemical Co. Two different sources (Aldrich and Fluka) of the templating agent, a 20% aqueous solution of tetrapropylammonium hydroxide (TPAOH), were used in order to compare the effect of alkali metal content on titanium incorporation in the product. The composition ratios used for synthesis of the titanium silicalite samples are given in Table I. In a typical experiment, 0.6 ml of TEOT was added dropwise to 40 ml of TEOS contained in a stirred PTFE autoclave liner kept under nitrogen. The clear yellow solution obtained was then mixed for a further 30–60 minutes before the dropwise addition of 30 ml of TPAOH. If, upon addition of the first few drops of TPAOH, the clear solution turned cloudy (as a white precipitate formed), further addition of TPAOH was only continued after the solution again became clear. When all the TPAOH had been added, the PTFE liner was transferred to a water bath maintained at 80°C and the solution was stirred for 3 hours. At the end of this time, the mixture was topped up to its original volume with deionised water and left to stir overnight. The Teflon liner was then transferred to a Parr autoclave reactor and crystallized for 96 hours at 175°C under autogenous pressure. The autoclave was cooled and the white gelatinous solution formed was then centrifuged at 20,000 rpm for 10 minutes. The supernatant liquid was discarded, deionised water added and the white deposit redispersed by sonicating for 5 minutes. The process was repeated 4–5 times until the pH of the supernatant solution was close to neutral. The final solution was dried at 80–90°C overnight and the resulting

TABLE I Composition measurements and estimates

Sample no	Precursor mole ratio		Ti : Si mole ratio		Atomic concentrations		
	Ti : Si	TPAOH : Si	EDX	XPS	$\left(\frac{460}{460 + 458}\right)_{\text{XPS}}$	$\left(\frac{(\text{Ti})\text{Tetra}}{\text{Si}}\right)_{\text{XPS}}$	$\left(\frac{960}{800}\right)_{\text{Raman}}$
19	0.0155	0.17	0.00958	0.0060	0.9827	0.0059	140
18	0.0155	0.26	0.0176	0.0072	0.8878	0.0064	105
17	0.0103	0.26	0.0127	0.0159	0.3255	0.0052	50
16	0.0155	0.17	0.0097	0.0067	0.8934	0.0060	150
15	0.0103	0.23	0.0086	0.0059	0.8393	0.0049	135
14	0.0103	0.34	0.0089	0.0061	0.9840	0.0060	133
13	0.0351	0.49	0.0209	0.0353	0.0415	0.0015	100
12	0.0310	0.49	0.0219	0.0138	0.7476	0.0103	150
11	0.0310	0.49	0.0196	0.0114	0.7027	0.0080	133
10	0.0310	0.49	0.0310	0.0296	0.1195	0.0035	88
9	0.0310	0.49	0.0226	0.0374	0.1894	0.0071	82
8	0.0103	0.34	0.0101	0.0137	0.1759	0.0024	53
7	0.0310	0.36	0.0307	0.0220	0.2566	0.0057	190
6	0.0103	0.34	0.0119	0.0070	0.9283	0.0065	150
5	0.0310	0.49	0.0284	0.0153	0.6293	0.0096	190
4	0.0310	0.49	0.0295	0.0186	0.5598	0.0104	167
3	0.0351	0.49	0.0196	0.0488	0.2160	0.0105	100
2	0.0351	0.49	0.0170	0.0494	0.2173	0.0107	50
1	0.0351	0.49	0.0201	0.0729	0.0067	0.0005	40

TABLE II Unit cell dimensions of selected TS-1 samples

Sample no	a (Å)	b (Å)	c (Å)	V_{cell} (Å ³)
ZSM-5 ^a	19.879	20.107	13.369	5343.684
TS-1 ^b	20.111	19.917	13.385	5361.372
2	20.065 ± 0.086	19.849 ± 0.129	13.367 ± 0.050	5323.655 ± 45.814
10	20.038 ± 0.064	19.866 ± 0.071	13.383 ± 0.031	5327.316 ± 28.875
13	20.052 ± 0.081	19.929 ± 0.066	13.375 ± 0.095	5344.540 ± 47.127
14	20.048 ± 0.117	20.030 ± 0.070	13.403 ± 0.065	5382.132 ± 44.835
18	20.032 ± 0.029	19.819 ± 0.017	13.483 ± 0.003	5352.472 ± 8.181
19	20.042 ± 0.015	19.889 ± 0.101	13.528 ± 0.062	5391.545 ± 44.157

^aSource: [24].^bSource: [10] data for 1.1% Ti.

white powder was then calcined in air at 550°C for 3–6 hours.

3. Results of characterisation

3.1. X-ray diffraction

Crystal structures of the powder products were identified by x-ray diffraction (XRD) using a Philips PW1831 diffractometer with Cu K_α radiation of wavelength 1.5418 Å. The spectra were recorded over the range of Bragg angles 10° ≤ 2θ ≤ 40° at a scanning rate of 0.01° per 10 seconds and the XRD patterns of some representative samples are presented in Fig. 1. In all cases, the patterns showed excellent evidence of MFI structure as well as high crystallinity under the synthesis conditions examined. In comparison with silicalite, the patterns of Ti-containing samples show a single diffraction peak at 2θ of 24.45°, indicating a change from a monoclinic symmetry (silicalite) to an orthorhombic symmetry (titanium silicalite, TS-1). No other phases were detected by XRD. The unit cell parameters of the samples were calculated using the program Traces (version 3.0) from Powder XRD Analytical Software taking several reflections of the XRD patterns and typical results are presented in Table II. The lattice parameters of the samples show enhanced values of the unit cell volume by about 30 to 50 Å³ in comparison with silicalite-1,

but are slightly larger than the values presented by Taramasso *et al.* [1]. Similar to other researchers, our calculated results also showed some dependence on the number of the selected reflections [20] as well as the angle step-size and integration time used for the XRD analysis—however a linear relationship between unit cell expansion and product titanium content [9] was not observed.

3.2. Electron diffraction X-ray analysis

The titanium-silicon atomic ratios in the solid products were obtained using Philips a XL30 scanning electron microscope equipped with an energy dispersive x-ray spectrometer and are presented in Table I for comparison with the precursor. From the data in Table I, it can be seen that the product Ti/Si ratio generally increases with concentration of titanium in the precursor, but is almost always lower than the same ratio in the synthesis solution. In most cases between 60 and 90% of the initial titanium content was found in the crystalline product. The implication that titanium species are incorporated less effectively than silicon in the zeolite framework agrees with the results of Tuel *et al.* [26] but contrasts with the enrichment reported by Van der Pol *et al.* [7] and Thangaraj *et al.* [6]. No definite correlation was observed between the TPAOH : Si ratio in

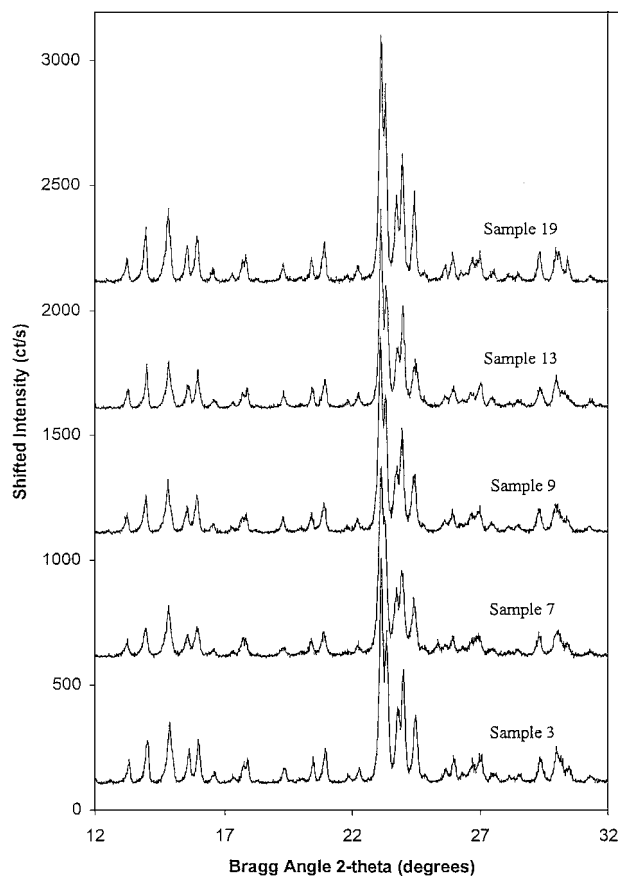


Figure 1 X-ray diffraction patterns for selected TS-1 samples.

the precursor and product titanium content. Other conditions being equal, a lower titanium content was generally observed for those materials prepared using Fluka rather than Aldrich TPAOH as the template. As a result of observations of the negative effects of alkali metals on TS-1 synthesis [1, 27], the alkali metal content of the two template solutions was measured using an inductively coupled plasma atomic emission spectrometer. The results showed that the Fluka TPAOH contained significantly more potassium ($54 \text{ mg} \cdot \text{dm}^{-3}$) and slightly more sodium ($3 \text{ mg} \cdot \text{dm}^{-3}$) than the Aldrich material (both metal ions $< 1 \text{ mg} \cdot \text{dm}^{-3}$).

3.3. Raman

Raman spectra of some representative samples are shown in Fig. 2. The spectra were measured using a Renishaw 3000 MicroRaman system equipped with an Olympus BH-2 microscope and the excitation source used was a 25 mW helium-neon laser ($\lambda = 632.8 \text{ nm}$). Raman spectroscopy is sensitive to low concentrations of both of the stable crystal phases of titanium dioxide, anatase and rutile [19, 36]. Raman spectra for anatase typically show four main peaks at 144 cm^{-1} , 638 cm^{-1} , 517 cm^{-1} and 396 cm^{-1} , in approximate order of intensity. Since anatase only begins to transform into rutile at relatively high temperatures (above 700°C), the spectral features of rutile—two main peaks at 446 cm^{-1} and 609 cm^{-1} , as well as a broad band at 238 cm^{-1} —were not expected to be present in any of the samples. As mentioned previously, the presence and intensity of the Raman band at 960 cm^{-1} is well correlated with titanium content in the silicalite framework [7, 13]. The Raman spectra for all the samples revealed a peak at

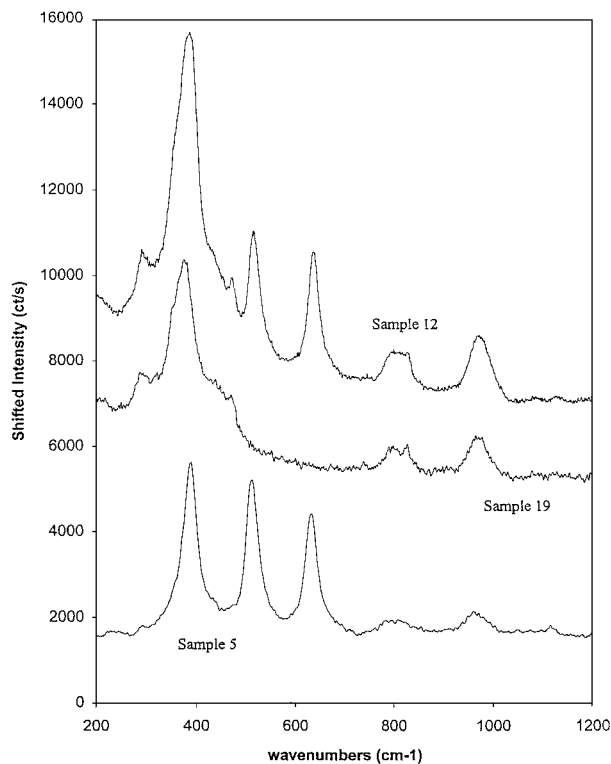


Figure 2 Raman spectra for selected TS-1 samples.

960 cm^{-1} , indicating titanium incorporation in the zeolite framework. Raman peaks corresponding to anatase were observed in only five materials—samples 4, 5, 7, 11 and 12—and no peaks corresponding to rutile were found. In each of these cases the synthesis solution contained Aldrich TPAOH and the mole ratio of titanium to silicon precursor was greater than 0.03—providing qualitative agreement with the limit suggested in the original patent [1].

In addition, the intensity of the 960 cm^{-1} peak relative to the 800 cm^{-1} Raman peak can be used to qualitatively estimate the efficiency of titanium incorporation. For the same TPAOH : Si and Ti : Si ratios, samples prepared using Fluka TPAOH as template, resulted in a lower relative intensity than those prepared using the Aldrich TPAOH, indicating lower titanium incorporation efficiency. This is considered to be related to the higher alkali metal content of the templating agent from Fluka [11, 38].

3.4. X-ray photoelectron spectroscopy

XPS analyses were performed using a Physical Electronics PHI5600 Surface Science Analysis System. A binding energy of 285.0 eV for C(1s) was chosen as an internal reference. Surface atomic compositions were estimated using the ratio between the areas of the peaks in photoelectron spectra and the sensitivity factors corresponding to the respective elements. XPS can provide information about the state and composition of the surface layer of zeolite crystals, penetrating to a depth of 4–5 nm. Earlier results obtained using both titania-silica mixed oxides [39, 40] and titanium silicalites [15, 41] have identified the photoelectron transition at 460 eV with titanium in a tetrahedral position (i.e., in the silicalite lattice), while the transition at 458 eV is identified with titanium species in

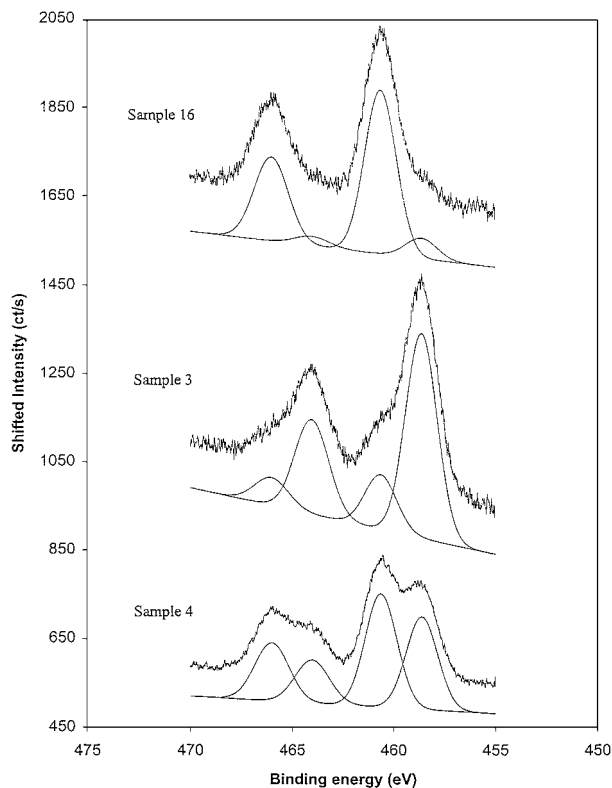


Figure 3 XPS results for TS-1 samples.

octahedral coordination (i.e. extra-framework anatase). Thus the concentration of titanium in different coordination states can be obtained and the signal intensity ratio, $Ti(2p)_{tetra} : Ti(2p)_{oct}$, can be used to estimate the ratio of framework to extra-framework titanium at the surface. Typical XPS spectra of some representative samples are shown in Fig. 3 and, in addition to the Ti : Si atomic concentration ratio, two intensity ratios are given in Table I for each sample, $Ti(2p)_{tetra}/(Ti(2p)_{oct} + Ti(2p)_{tetra})$ and $Ti(2p)_{tetra} : Si$.

In terms of the Ti : Si mole ratio, it is clear that the source of templating agent has a significant effect. The XPS results plainly demonstrate that all the samples produced using TPAOH from Aldrich have surface Ti : Si ratios lower than those in both the bulk solid (EDX) and the synthesis solution. Vetter *et al.* also observed a low titanium concentration in the surface layer of their TS-1 samples than that measured by atomic absorption spectroscopy (AAS) [28]. Those samples produced from Fluka TPAOH however, typically have surface Ti : Si ratios greater than or similar in value to the synthesis solution and, in most cases, greater than in the bulk solid (EDX).

Although not observed in many of the Raman spectra, the XPS results indicate that some octahedrally coordinated (extra-framework) titanium species were still present in the surface of all the products. The $Ti(2p)_{tetra}/(Ti(2p)_{oct} + Ti(2p)_{tetra})$ ratio appears to provide further evidence of the effect of alkali metal ions on the zeolite surface composition: for samples produced using TPAOH from Fluka, the *maximum* fraction of surface titanium in tetrahedral coordination was 0.3255 for sample 17 whereas for those produced using TPAOH from Aldrich, all but one of them (sample 7) contained over 55% of surface titanium in tetrahedral coordina-

tion. The dramatic difference in both the concentration of the two titanium coordination states at the surface and the titanium concentration gradient from surface to bulk solid suggests that the difference in templating agent has a significant impact on the processes involved in titanium incorporation in the zeolite framework.

The third ratio calculated from the XPS results, $Ti(2p)_{tetra} : Si$, indicates the actual extent of titanium incorporation in the surface silicalite layer. The maximum value observed was approximately 1%, although for those samples with the highest fractions of surface titanium in tetrahedral coordination—samples 6, 14 and 19—the surface titanium to silicon atomic ratio was only 0.6–0.7%.

3.5. Nitrogen Adsorption

The samples' specific surface areas were measured based on the Brunauer-Emmett-Teller (BET) isotherm using a Micromeritics ASAP 2000 nitrogen adsorption apparatus and the results are presented in Table III. While all the measured surface areas are within the range stated in Taramasso *et al.*'s 1987 patent [37], the data presented again demonstrate a difference based on the templating agent used. The average specific surface area for those TS-1 samples prepared using TPAOH containing a low concentration of alkali metal cations is approximately $350 \text{ m}^2 \cdot \text{g}^{-1}$, whereas for materials produced using an ultra low alkali metal content TPAOH the average is approximately $440 \text{ m}^2 \cdot \text{g}^{-1}$. Given that the XRD results show that the two groups of materials have the same structure and that no other crystal phases are present in significant quantities, the reduced surface areas can only be due either to severe restriction or blockage of the zeolite pores and channels.

4. Mechanism of formation of crystals of varying spatial composition

The initial steps in the synthesis of crystalline TS-1 zeolite involve a titanium alkoxide (TEOT) being diluted into the silica source (TEOS), which initially acts

TABLE III Specific surface areas of TS-1 samples

Sample no	TPAOH source	Calcination time (days) ^a	BET surface area (m ² /g)
1	Fluka	2.7	355.8 ± 3.10
2	Fluka	3.5	366.8 ± 0.83
3	Fluka	2	364.1 ± 1.73
4	Aldrich	2	436.5 ± 11.06
5	Aldrich	1	442.1 ± 9.46
6	Aldrich	4	463.8 ± 7.91
7	Aldrich	4	451.7 ± 8.36
8	Fluka	4	358.8 ± 6.55
9	Fluka	4	365.1 ± 0.72
10	Fluka	2	364.0 ± 0.41
11	Aldrich	2	437.5 ± 9.0
12	Aldrich	2	430.3 ± 10.3
13	Fluka	2	310.3 ± 1.46
14	Aldrich	4	450.3 ± 7.10
15	Aldrich	2	450.6 ± 6.60
16	Aldrich	2	439.4 ± 8.70
17	Fluka	2	348.0 ± 6.1
18	Aldrich	4	447.4 ± 8.65
19	Aldrich	4	449.2 ± 4.7

^aAll the samples were calcined at 550°C.

as a solvent, followed by the addition of an aqueous solution of a basic templating agent (TPAOH) to perform hydrolysis of the alkoxides. Prior to hydrolysis, Kraushaar proposed that all titanium in the mixture should be present as single titanium alkoxide units in mixed oligomers with the silicon alkoxide [29]. In the presence of TPAOH however, the silicon alkoxides are present mostly as monomers and the titanium alkoxides are present mostly as trimers [9]. The resulting silica-titana hydrogel which forms is always supersaturated with respect to the concentration of its chemical constituents and in a disordered state with higher entropy than its ordered counterpart, the crystallised zeolite structure. In such a labile system, many factors can provoke phase transformation. Under hydrothermal conditions this supersaturation is removed through nucleation of the metastable zeolite phase. After nucleation, other processes occur in parallel with crystal growth including gel dissolution and re-crystallisation. According to the Ostwald-Thomson relation, the formation of the gel skeleton and crystal nuclei from the solution of colloidal particles depends on the dimensions of the particles, e.g. particles smaller than a critical size will dissolve, those larger than the critical size will grow further. Both the composition and proportions of these phases can be expected to vary continuously during the course of crystallisation. Therefore, there are ample opportunities afforded for substitution of one ion for another during the dynamics of crystallisation. Furthermore, the inhomogeneity of reactants during nucleation or differences in rates of dissolution of reagents might cause spatial composition variations within the crystal during its growth, as has been reported for both X and ZSM-5 zeolite crystals [30].

Depending on the initial concentration of titanium alkoxide, the reaction mixture would probably contain a distribution of different titanium alkoxide oligomers in equilibrium. At low concentrations, the titanium species is most probably present as single titanium alkoxide monomers, in a relatively homogeneous dispersion in the silicon alkoxide, leading to the formation of Si—O—Ti—O—Si bonds instead of Ti—O—Ti bonds on hydrolysis. Therefore, at the beginning of crystallization, titanium could be incorporated into the MFI silicalite framework at a maximum concentration. As the crystals grow, the concentration of titanium species in the hydrogel would gradually reduce due to their incorporation in the tetrahedral framework and thus the Ti/Si ratio in the peripheral parts of the crystals would decrease relative to the bulk. Hence the heterogeneity of the zeolite crystal growth in the gel would be determined by changes in composition of the liquid phase of the gel throughout its crystallization. As a result, a progressive reduction of the Ti/Si ratio from the centre to the surface of the crystal could be observed.

This does not necessarily preclude the formation of non-framework Ti species however. The experimental results have shown that in most cases the titanium content in crystalline product was lower than that of the precursor mixture. It is possible that small quantities of unassociated monomers or oligomers could lead to aggregated oxide phases upon hydrolysis and deposi-

tion in the surface as extraframework titanium species, as observed by XPS spectroscopy. This could explain why complete incorporation of all the titanium into the structural framework was not obtained even in the precursor solution with the Ti/Si ratio of 0.0103.

At higher titanium concentrations, the distribution of titanium alkoxide oligomers in the initial mixture could shift towards more dimers. As described above, the formation of nuclei and growth of crystals are closely related to the concentration of the components in the synthesis solution, and thus to the dissolubility of the components. The aggregation of such higher titanium oligomer species could result in the formation of an amorphous phase upon hydrolysis, and ultimately anatase, which would not redissolve.

5. Conclusions

This paper has presented an investigation into the effect of synthesis mixture composition on the physical characteristics of titanium silicalite (TS-1). Across the range of compositions studied, x-ray diffraction indicated that all the samples had the MFI crystalline structure and, together with Raman, demonstrated incorporation of titanium in the zeolite framework. Energy dispersive x-ray analysis showed that those samples produced using an ultra-low alkali metal content templating agent generally resulted in a higher degree of titanium incorporation in the zeolite framework and XPS showed the same samples to have both a lower titanium surface concentration and a higher proportion of titanium incorporation in the surface. A simplified mechanism to explain this composition variation was proposed. The reduction in specific surface areas observed for samples produced using the templating agent with a relatively higher alkali metal content was postulated to be due to blocked zeolite pores and channels as a result of the formation of extra-framework crystallites.

Acknowledgements

The authors would like to thank the Research Grants Council of Hong Kong for their financial support through RGC grant HKUST 663/96P.

References

1. M. TARMASSO, G. PEREGO and B. NOTARI, U.S. Patent 4,410,501 (1983).
2. A. ESPOSITO, C. NERI, F. BUONOMO and M. TARMASSO, U.K. Patent 2,116,974B (1985).
3. P. ROFFIA, G. MANTEGAZZA, M. PADOVAN, G. PETRINI, S. TONTI and P. GERVA SUTTI, *Stud. Surf. Sci. Catal.* **55** (1990) 43.
4. U. ROMANO, A. ESPOSITO, F. MASPERO, C. NERI and M. G. CLERICI, *Stud. Surf. Sci. Catal.* **55** (1990) 33.
5. M. G. CLERICI, *Appl. Catal.* **68** (1991) 249.
6. A. THANGARAJ, S. SIVASANKER and P. RATNASAMY, *J. Catal.* **131** (1991) 294.
7. A. J. H. P. VAN DER POL and J. H. C. VAN HOOFF, *Appl. Catal. A* **92** (1992) 93.
8. F. MASPERO and U. ROMANO, *J. Catal.* **146** (1994) 476.
9. A. THANGARAJ, M. J. EAPEN, S. SIVASANKER and P. RATNASAMY, *Zeolites* **12** (1992) 943.
10. R. MILLINI, E. PREVIDE MASSARA, G. PEREGO and G. BELLUSSI, *J. Catal.* **137** (1992) 497.

11. B. NOTARI, *Stud. Surf. Sci. Catal.* **37** (1988) 413.
12. C. B. KHOUW, C. B. DARTT, J. A. LABINGER and M. E. DAVIS, *J. Catal.* **149** (1994) 195.
13. G. PEREGO, G. BELLUSSI, C. CORDO, M. TARMASSO, F. BUONOMO and A. ESPOSITO, *Stud. Surf. Sci. Catal.* **28** (1986) 129.
14. D. R. C. HUYBRECHTS, L. DE BRUYCKER and P. A. JACOBS, *J. Mol. Catal.* **71** (1992) 184.
15. G. DEO, A. M. TUREK, I. E. WACHS, D. R. C. HUYBRECHTS and P. A. JACOBS, *Zeolites* **13** (1993) 365.
16. M. G. CLERICI and P. INGALLINA, *J. Catal.* **140** (1993) 71.
17. A. THANGARAJ, R. KUMAR, S. P. MIRAJKAR and P. RATNASAMY, *J. Catal.* **130** (1991) 1.
18. M. A. CAMBLOR, A. CORMA and J. PEREZ-PARIENTE, *Zeolites* **13** (1993) 82.
19. G. BUSCA, G. RAMIS, J. M. GALLARDO AMORES, V. SANCHEZ ESCRIBANO and P. PIAGGIO, *J. Chem. Soc. Faraday Trans.* **90** (1994) 3181.
20. R. MILLINI, E. PREVIDE MASSARA, G. PEREGO and G. BELLUSSI, *J. Catal.* **68** (1992) 479.
21. D. TRONG ON, I. DENIS, C. LORTIE, C. CARTIER and L. BONNEVIOT, *Stud. Surf. Sci. Catal.* **83** (1994) 101.
22. P. BEHRENS, J. FELSCHE, S. VETTER, G. SCHULZ-ELKOFF, N. I. JAEGER and W. NIEMANN, *J. Chem. Soc. Chem. Commun.* **10** (1991) 678.
23. G. N. VAYSSILOV, *Catal. Rev.-Sci. Eng.* **39**(3) (1997) 209.
24. M. M. J. TREACY, J. B. HIGGINS and R. VON BALLMOOS, in "Collection of Simulated XRD Powder Diffraction Patterns for Zeolites", third edition (revised). (1996) Elsevier, London.
25. A. TUEL and Y. BEN TAARIT, *Zeolites* **14** (1994) 272.
26. *Idem.*, *Applied Catalysis A* **110** (1994) 137.
27. G. BELLUSSI and V. FATTORE, *Stud. Surf. Sci. Catal.* **69** (1991) 79.
28. S. VETTER, G. SCHULZ-EKLOFF, K. KULAWIK and N. I. JAEGER, *Chem. Eng. Technol.* **17** (1994) 348.
29. B. KRAUSHAAR, Ph.D. Thesis, Eindhoven University of Technology, 1989.
30. R. VON BALLMOOS and W. M. MEIER, *Nature* **389** (1981) 782.
31. G. ZHANG, J. STERTE and B. J. SCHOEMAN, *Chem. Mater.* **9** (1997) 210.
32. R. J. DAVIS, Z. LIU, J. E. TABORA and W. S. WIELAND, *Catal. Lett.* **34** (1995) 101.
33. E. ASTORINO, J. B. PERI, R. J. WILLEY and G. BUSCA, *J. Catal.* **157** (1995) 482.
34. A. ZECCHINA, G. SPOTO, S. BORDIGA, A. FERRERO, G. PETRINI, G. LEOFANTI and M. PADOVAN, *Stud. Surf. Sci. Catal.* **69** (1991) 251.
35. E. DUPREY, P. BEAUNIER, M.-A. SPRINGUEL-HUET, F. BOZON-VERDURAZ, J. FRAISSARD, J.-M. MANOLI and J.-M. BREGEAULT, *J. Catal.* **165** (1997) 22.
36. Y.-H. ZHANG, C. K. CHAN, J. F. PORTER and W. GUO, *J. Mater. Res.* **13**(9) (1998) 2602.
37. M. TARMASSO, G. MANARA, V. FATTORE and B. NOTARI, U.S. Patent 4,666,692 (1987).
38. G. BELLUSSI, A. CARATI, M. G. CLERICI and A. ESPOSITO, *Stud. Surf. Sci. Catal.* **63** (1991) 421.
39. S. M. MUKHOPAHYAY and S. H. GAROFALINI, *J. Non-Crystal. Solids* **126** (1990) 202.
40. A. Y. STAKHEEV, E. S. SHPIRO and J. APIJOK, *J. Phys. Chem.* **97** (1993) 5668.
41. D. TRONG ON, L. BONNEVIOT, A. BITTAR, A. SAYARI and S. KALIAGUINE, *J. Mol. Catal.* **74** (1992) 233.

Received 18 September 2001
and accepted 30 January 2002